Incoherent bremsstrahlung in nuclei

A. Gil, E. Oset

*Departamento de Física Teórica and IFIC, Centro Mixto Universidad de Valencia-CSIC,
E-46100 Burjasot, Valencia, Spain*

Received 29 June 1994

Abstract

We have studied the processes $A(e, e'\gamma)X$ in nuclei, or incoherent bremsstrahlung, and determined expressions for the cross section in terms of the same nuclear response functions R_L, R_T, which appear in inclusive electron scattering (e, e') in nuclei. Calculations of the cross sections are carried out using a Fermi gas model, complemented by the local-density approximation, to evaluate the response functions. We have carried out a study which shows that the reaction can be used to determine reliably the response functions from experimental data. On the other hand we have compared the incoherent bremsstrahlung with the coherent one in order to see the limits to the tagging technique, which produces monochromatic photons based on the assumption of the dominance of the coherent process. We observe that at energies $E_\gamma < 1$ GeV the dominance of the coherent process extends to relatively large scattering angles, making the present technique completely safe. However, as the energy of the electron increases, the region of dominance of the coherent process is reduced to smaller scattering angles. These results should be of use when extending the tagging technique to planned or future electron facilities.

1. Introduction

Ordinary bremsstrahlung (CB) in electron scattering from nuclei, $A_{g.s.}(e, e'\gamma)$ $A_{g.s.}$, is a coherent process from the nuclear point of view. The nucleus does not break and remains in its ground state. Consequently all protons contribute coherently to the amplitude and the process shows a Z^2 dependence. For low electron energies compared to typical nuclear excitation energies, this process is obviously the only one which can occur to produce a photon.

However, as the energy of the electron increases, and becomes large compared to the nuclear excitation energies, there is no problem in principle to transfer some energy to the nucleus at the same time that a photon is produced. This would lead

to nuclear excited levels or breakup in the continuum and it would constitute what we call here the incoherent bremsstrahlung (IB).

There are two reasons which have led us to make a study of this process:

(i) The tagging technique to produce monochromatic photon beams assumes implicitly that all the photons are produced in the CB. Hence, the energy of the photon is directly given by the difference of energies between the initial and final electron (neglecting a small nucleus recoil energy). Also the CB produces photons in a narrow beam along the direction of the e^- momentum transfer.

As the energy of the e^- increases, the proportion of IB is bound to increase and at certain energies and certain kinematical conditions it can compete or even dominate over the coherent process. This sets the limits to the tagging technique, since if the incoherent process dominates we do no longer know the energy and direction of the photons.

It is thus very useful for experimental purposes to know where these limits appear.

(ii) In the study of the IB we find that the cross section can be written as a linear combination of the longitudinal and transverse response functions which appear in inclusive (e, e') experiments. The discrepancy of theoretical models with the longitudinal response function has been a constant in time, though many theoretical papers have been devoted to unraveling this puzzle. Recently some more wood has been added to the fire with the measurement at BATES of the response functions [1] which show a large discrepancy with previous determinations of the longitudinal response at Saclay [2] and would be in better agreement with standard calculations.

In view of these large discrepancies with the same type of experiment, alternative experiments which provide this information should be welcome.

Although the cross sections in IB are of the order α with respect to those in the (e, e') experiments, one has the advantage that one can determine the two structure functions over a wide domain of $(\omega, |q|)$ without changing the energy of the initial electron beam, only playing with the energy and direction of the final electron and photon. This is not the case in the (e, e') experiments which require one to change the energy of the initial electron beam, with obvious experimental inconveniences and additional problems of calibration [3].

In this paper we compare the IB to the CB for different energies of the e^- beam and different kinematical situations. On the other hand we investigate the optimal kinematical situations where, by means of two measurements of the cross sections, one can obtain two independent equations which determine W_L and W_T with minimum error. This should serve as a guideline for experiments trying to determine the response functions from IB.

2. Coherent bremsstrahlung in nuclei

The CB is a well-known process and a part of text books [4,5]. The Feynman diagrams which contribute to the process are shown in Fig. 1. The cross section is
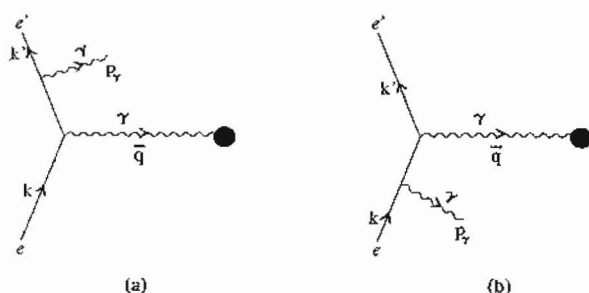
Fig. 1. Feynman diagrams for the coherent bremsstrahlung.

given by

$$
\begin{aligned}
\frac{d^3\sigma}{dE_\gamma \, d\Omega_\gamma \, d\Omega_{out}} \\
= \frac{\alpha^3 Z^2 [F(q)]^2 |p_\gamma| |k'|}{2\pi^2 |k| |q|^4} \Bigg\{ \frac{1}{(p_\gamma \cdot k)^2} \Big\{ 2p_\gamma^0 k'^0 \big[(p_\gamma \cdot k) + m^2\big] \\
- 2k'^0 k^0 \big[(p_\gamma \cdot k) + m^2\big] - 2(k^0)^2(p_\gamma \cdot k) + 2(p_\gamma \cdot k)(k \cdot k') \\
- (p_\gamma \cdot k')(p_\gamma \cdot k) + m^2\big[(k' \cdot k) + (p_\gamma \cdot k) - (p_\gamma \cdot k')\big] - m^4 \Big\} \\
+ \frac{1}{(p_\gamma \cdot k')^2} \Big\{ 2p_\gamma^0 k^0 \big[(p_\gamma \cdot k') - m^2\big] + 2k'^0 k^0 \big[(p_\gamma \cdot k') - m^2\big] \\
+ 2(k'^0)^2 (p_\gamma \cdot k') - 2(p_\gamma \cdot k')(k \cdot k') - (p_\gamma \cdot k')(p_\gamma \cdot k) \\
+ m^2\big[(k' \cdot k) + (p_\gamma \cdot k) - (p_\gamma \cdot k')\big] - m^4 \Big\} + \frac{2}{(p_\gamma \cdot k)(p_\gamma \cdot k')} \\
\times \Big[p_\gamma^0 k^0 (k' \cdot k) + 2k'^0 k^0 (k' \cdot k) - p_\gamma^0 k'^0 (k' \cdot k) - (p_\gamma^0)^2 m^2 \\
- (k \cdot k')^2 + m^2 (k' \cdot k) \Big] \Bigg\},
\end{aligned}
\tag{1}
$$

with

$$
k^0 = k'^0 + p_\gamma^0,
$$

$$
|q| = |k - p_\gamma - k'|,
$$

$$
F(q) = \int d^3x \, \rho(x) \, e^{-iq \cdot x},
\tag{2}
$$

where $F(q)$ is the nuclear form factor and the variables are specified in Fig. 1.

Lorentz covariance and gauge invariance allows one to write

$$W'^{\mu\nu} = \frac{W^{\mu\nu}}{2\pi} = \left(\frac{q^{\mu}q^{\nu}}{q^2} - g^{\mu\nu}\right)W_1 + \left(P^{\mu} - \frac{(P\cdot q)}{q^2}q^{\mu}\right)\left(P^{\nu} - \frac{(P\cdot q)}{q^2}q^{\nu}\right)\frac{W_2}{M_A^2}$$

(5)

by means of which the cross section is given as

$$\frac{d^2\sigma}{d\Omega_{out}\,dE_{out}} = \frac{\alpha^2}{4E_{in}^2\sin^4(\frac{1}{2}\theta)}\left[2\sin^2(\tfrac{1}{2}\theta)W_1 + \cos^2(\tfrac{1}{2}\theta)W_2\right].$$

(6)

In a frame where the nucleus is at rest and γ is chosen along the z direction we have

$$W'^{xx} = W'^{yy} = W_1,$$

$$W'^{zz} = \frac{\omega^2}{q^2}\left(W_1 + \frac{|q|^2}{q^2}W_2\right),$$

$$W'^{ij} = 0 \quad (i \neq j) \quad i, j = 1, 2, 3.$$

(7)

Alternatively we can use the longitudinal and transverse response functions W_1, W_T as

$$W_L = -\frac{q^2}{\omega^2}W'^{zz} = -\frac{q^2}{|q|^2}W'^{00},$$

$$W_T = W'^{xx},$$

(8)

and the cross section is written in terms of them as

$$\frac{d^2\sigma}{d\Omega_{out}\,dE_{out}} = \frac{d\sigma}{d\Omega}\bigg|_{Mott}\frac{-q^2}{|q|^2}\left(W_L(\omega, |q|) + \frac{W_T(\omega, |q|)}{\epsilon}\right),$$

(9)

with

$$q^2 = \omega^2 - |q|^2,$$

$$\frac{d\sigma}{d\Omega}\bigg|_{Mott} = \frac{\alpha^2\cos^2(\frac{1}{2}\theta)}{4E_{in}^2\sin^4(\frac{1}{2}\theta)},$$

$$\epsilon = \left(1 - 2\frac{|q|^2}{q^2}\tan^2(\tfrac{1}{2}\theta)\right)^{-1}.$$

(10)

In order to obtain the hadronic tensor $W'^{\mu\nu}$, we evaluate it for a Fermi sea of nucleons [8,9] but use the local-density approximation to determine it in finite nuclei. We find

$$W'^{\mu\nu} = -\frac{1}{\pi e^2}\int d^3r\,\mathrm{Im}\,\Pi^{\mu\nu}(\rho(r)),$$

(11)
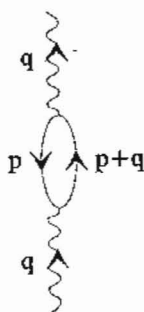
Fig. 3. Self-energy Feynman diagram of the photon corresponding to the excitation of a particle–hole pair.

where $\Pi^{\mu\nu}$ is the polarization tensor of the Fermi sea due to particle–hole excitation induced by an external photon, Fig. 3,

$$
\begin{aligned}
&-i\Pi^{\mu\nu}(q) \\
&= -ie^2 \int \frac{d^3p}{(2\pi)^3} \frac{n(p)[1 - n(p+q)]}{\omega + E(p) - E(p+q) + i\eta} \mathrm{Tr}\, \mathscr{A}^{\mu\nu} \frac{M}{E(p)} \frac{M}{E(p+q)},
\end{aligned}
\tag{12}
$$

where

$$
\begin{aligned}
\mathscr{A}^{\mu\nu} &\equiv \frac{\not{p} + M}{2M} \left[\gamma^\mu F_1(q^2) + F_2(q^2) \left(-\frac{(2p+q)^\mu}{2M} + \gamma^\mu \right) \right] \\
&\times \frac{\not{p} + \not{q} + M}{2M} \left[\gamma^\nu F_1(q^2) + F_2(q^2) \left(-\frac{(2p+q)^\nu}{2M} + \gamma^\nu \right) \right].
\end{aligned}
\tag{13}
$$

By evaluating the trace of $\mathscr{A}^{\mu\nu}$ and the imaginary part of $\Pi^{\mu\nu}$ we obtain

$$
\begin{aligned}
\mathrm{Im}\, \Pi^{\mu\nu} &= -\pi e^2 \int \frac{d^3p}{(2\pi)^3} \frac{n(p)[1 - n(p+q)]}{E(p)E(p+q)} \delta(\omega - E(p+q) + E(p)) \\
&\times \left[A_1 \left(2p^\mu p^\nu + p^\mu q^\nu + \tfrac{1}{2} q^2 g^{\mu\nu} + p^\nu q^\mu \right) + A_2 (2p+q)^\mu (2p+q)^\nu \right. \\
&\left. + A_3 (2p+q)^\mu (2p+q)^\nu \left(2 - \frac{q^2}{2M^2} \right) \right],
\end{aligned}
\tag{14}
$$

where

$$
\begin{aligned}
A_1 &\equiv \left[F_1^{pr}(q^2) + F_2^{pr}(q^2) \right]^2 + \left[F_1^n(q^2) + F_2^n(q^2) \right]^2, \\
A_2 &\equiv \left\{ -F_1^{pr}(q^2) F_2^{pr}(q^2) - \left[F_2^{pr}(q^2) \right]^2 \right\} + \left\{ -F_1^n(q^2) F_2^n(q^2) - \left[F_2^n(q^2) \right]^2 \right\}, \\
A_3 &\equiv \tfrac{1}{4} \left\{ \left[F_2^{pr}(q^2) \right]^2 + \left[F_2^n(q^2) \right]^2 \right\}.
\end{aligned}
\tag{15}
$$

Particularizing for Π^{00} and Π^{xx} and taking the approximations in $\mathscr{A}^{\mu\nu}$

$$p^0 \approx M\left(1 + \frac{3K_F^2}{10M^2}\right), \quad (p^x)^2 \approx \tfrac{1}{3}K_F^2, \tag{16}$$

we obtain finally

$$W_L = -\frac{q^2}{|q|^2}\int \frac{d^3r}{(2\pi)^2}\int_0^{K_F} \frac{|p|\,d|p|}{|q|E(p)}\Theta(1 - |\cos\theta|)\Theta(|q+p|-K_F)\mathscr{F}(q),$$

$$W_T = \int \frac{d^3r}{(2\pi)^2}\int_0^{K_F} \frac{|p|\,d|p|}{|q|E(p)}\Theta(1 - |\cos\theta|)\Theta(|q+p|-K_F)\mathscr{H}(q), \tag{17}$$

with

$$\cos\theta = \frac{\omega^2 - |q|^2 + 2\omega E(p)}{2|p||q|},$$

$$\mathscr{H}(q) = A_1\left(\tfrac{2}{3}K_F^2 - \tfrac{1}{2}q^2\right) + A_2\cdot\tfrac{4}{3}K_F^2 + A_3\cdot\tfrac{4}{3}K_F^2\left(2 - \frac{q^2}{2M^2}\right),$$

$$\mathscr{F}(q) = A_1\left[2\left(M + \frac{3K_F^2}{10M}\right)^2 + 2\left(M + \frac{3K_F^2}{10M}\right)\omega + \frac{q^2}{2}\right]$$

$$+ A_2\left[2\left(M + \frac{3K_F^2}{10M}\right) + \omega\right]^2 + A_3\left[2\left(M + \frac{3K_F^2}{10M}\right) + \omega\right]^2\left(2 - \frac{q^2}{2M^2}\right). \tag{18}$$

Our approach improves over the Fermi sea approach using a fixed average momentum [9], and this procedure of using a Fermi sea, complemented by the local-density approximation, has proved very accurate in describing processes like μ^- capture or ν scattering in nuclei [10,11].

In Fig. 4 we compare our results with experiment in ^{40}Ca using the data of Refs. [1,2]. We have also included the effect of the Q value for the nuclear breakup, by subtracting 12 MeV from the photon energy, which is the average excitation energy needed to create n^{39}Ca or p^{39}K. As we can see, we get a reasonable description of R_T (defined in terms of W_T as $R_T = 2W_T$) if one recalls that we do not consider Δh excitations, which fill the high-energy part of the spectrum. Our results for R_L (in terms of W_L, $R_L = -(|q|^2/q^2)W_L$) are in disagreement with the data of Ref. [2], like the majority of the theoretical approaches, but much closer to those of Ref. [1].

In any case, the accuracy of the response functions is sufficiently good to make use of them in the study of the IB of the next section.
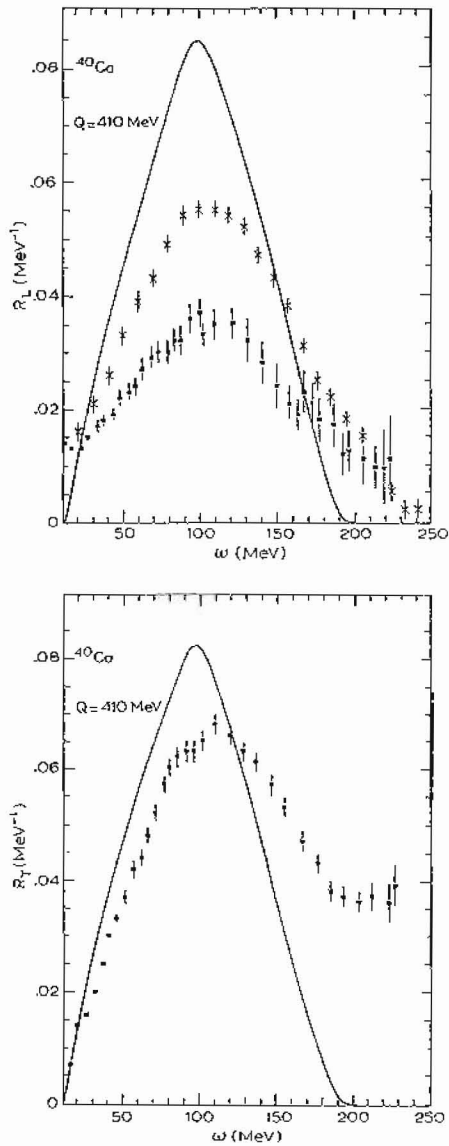
Fig. 4. Response functions: comparison between experimental (the "x" points are from BATES and the solid squares from Saclay) and our theoretical results.

4. Incoherent bremsstrahlung

The process we study now is $A(e, e'\gamma)X$, which in the approximation of one-photon exchange is depicted in Fig. 5.
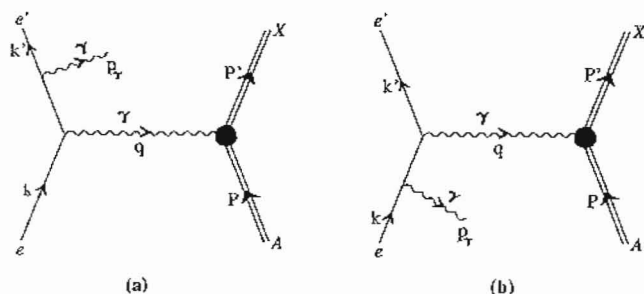
Fig. 5. Feynman diagrams considered for the incoherent bremsstrahlung.

The cross section for this process is written as

$$\frac{d^4\sigma}{d\Omega_{out}\, dE_{out}\, d\Omega_\gamma\, dE_\gamma} = \frac{\alpha^3 m^2 |k'|\,|p_\gamma|}{2\pi^3 |k|\, q^4} L^{\mu\nu} W_{\mu\nu},\tag{19}$$

where $W_{\mu\nu}$ is the same hadronic tensor as found in the former section and $L^{\mu\nu}$ is the new leptonic tensor given by

$$
\begin{aligned}
L^{\mu\nu} &= \frac{1}{2}\sum_{s,r,r'}\left[\bar{u}_{r'}(k')\left(\not{\epsilon}_s\frac{\not{p}_\gamma+\not{k}'+m}{2(p_\gamma\cdot k')}\gamma^\mu+\gamma^\mu\frac{-\not{p}_\gamma+\not{k}+m}{-2(p_\gamma\cdot k)}\not{\epsilon}_s\right)u_r(k)\right]\\
&\quad\times\left[\bar{u}_r(k)\left(\gamma^\nu\frac{\not{p}_\gamma+\not{k}'+m}{2(p_\gamma\cdot k')}\not{\epsilon}_s+\not{\epsilon}_s\frac{-\not{p}_\gamma+\not{k}+m}{-2(p_\gamma\cdot k)}\gamma^\nu\right)u_{r'}(k')\right]\\
&= -\frac{1}{2}\operatorname{Tr}\left[\frac{\not{k}'+m}{2m}\left(\gamma_\rho\frac{\not{p}_\gamma+\not{k}'+m}{2(p_\gamma\cdot k')}\gamma^\mu+\gamma^\mu\frac{-\not{p}_\gamma+\not{k}+m}{-2(p_\gamma\cdot k)}\gamma_\rho\right)\right.\\
&\quad\left.\times\frac{\not{k}+m}{2m}\left(\gamma^\nu\frac{\not{p}_\gamma+\not{k}'+m}{2(p_\gamma\cdot k')}\gamma^\rho+\gamma^\rho\frac{-\not{p}_\gamma+\not{k}+m}{-2(p_\gamma\cdot k)}\gamma^\nu\right)\right].
\end{aligned}\tag{20}
$$

The explicit evaluation of the trace in Eq. (20) gives

$$
\begin{aligned}
L^{\mu\nu} &= \frac{1}{2m^2(p_\gamma\cdot k')^2(p_\gamma\cdot k)^2}\Big((p_\gamma^\mu k^\nu+p_\gamma^\nu k^\mu)\big\{(p_\gamma\cdot k)^2\big[(p_\gamma\cdot k')-m^2\big]\\
&\quad+(p_\gamma\cdot k')(p_\gamma\cdot k)(k\cdot k')\big\}+(k'^\mu k^\nu+k'^\nu k^\mu)\big[-m^2(p_\gamma\cdot k)^2\\
&\quad-m^2(p_\gamma\cdot k')^2+(p_\gamma\cdot k')(p_\gamma\cdot k)\big[2(k'\cdot k)+(p_\gamma\cdot k)-(p_\gamma\cdot k')\big]\big]\\
&\quad+\big(p_\gamma^\mu k'^\nu+p_\gamma^\nu k'^\mu\big)\big\{(p_\gamma\cdot k')^2\big[(p_\gamma\cdot k)+m^2\big]\\
&\quad-(p_\gamma\cdot k')(p_\gamma\cdot k)(k\cdot k')\big\}+2k'^\mu k'^\nu(p_\gamma\cdot k')(p_\gamma\cdot k)^2\\
&\quad-2k^\mu k^\nu(p_\gamma\cdot k')^2(p_\gamma\cdot k)-2p_\gamma^\mu p_\gamma^\nu(p_\gamma\cdot k')(p_\gamma\cdot k)m^2
\end{aligned}
$$

$$
\begin{aligned}
+ g^{\mu\nu}\Big[&(p_\gamma \cdot k')^2 (k' \cdot k) m^2 - (p_\gamma \cdot k')^3 (p_\gamma \cdot k) + (p_\gamma \cdot k')^2 (p_\gamma \cdot k) m^2 \\
&- (p_\gamma \cdot k')^3 m^2 - (p_\gamma \cdot k')^2 m^4 - 2(p_\gamma \cdot k')(p_\gamma \cdot k)(k \cdot k')^2 \\
&- 2(p_\gamma \cdot k')(p_\gamma \cdot k)^2 (k \cdot k') + 2(p_\gamma \cdot k')^2 (p_\gamma \cdot k)(k \cdot k') \\
&+ 2(p_\gamma \cdot k')(p_\gamma \cdot k)(k \cdot k') m^2 + (p_\gamma \cdot k)^2 (k' \cdot k) m^2 - (p_\gamma \cdot k')(p_\gamma \cdot k)^3 \\
&+ (p_\gamma \cdot k)^3 m^2 - (p_\gamma \cdot k')(p_\gamma \cdot k)^2 m^2 - (p_\gamma \cdot k)^2 m^4 \Big]\Big).
\end{aligned}
\tag{21}
$$

And recalling Eq. (5) we can write

$$
\frac{d^4\sigma}{d\Omega_{\text{out}}\, dE_{\text{out}}\, d\Omega_\gamma\, dE_\gamma} = \frac{\alpha^3 |k'|\,|p_\gamma|}{2\pi^2 |k|\, q^4 (p_\gamma \cdot k')^2 (p_\gamma \cdot k)^2}\,(W_1 C_1 + W_2 C_2),
\tag{22}
$$

where C_1 and C_2 are given by

$$
\begin{aligned}
C_1 = 2\Big[&(p_\gamma \cdot k')(p_\gamma \cdot k)^3 - (p_\gamma \cdot k)^3 m^2 + 2(p_\gamma \cdot k')(p_\gamma \cdot k)^2 (k \cdot k') \\
&- 2(p_\gamma \cdot k')^2 (p_\gamma \cdot k)(k \cdot k') + (p_\gamma \cdot k')^3 (p_\gamma \cdot k) + (p_\gamma \cdot k')^3 m^2 \\
&- (p_\gamma \cdot k)^2 (k \cdot k') m^2 + 2(p_\gamma \cdot k')(p_\gamma \cdot k)(k \cdot k')^2 \\
&- (p_\gamma \cdot k')^2 (k \cdot k') m^2 - (p_\gamma \cdot k')^2 (p_\gamma \cdot k) m^2 + 2(p_\gamma \cdot k)^2 m^4 \\
&+ (p_\gamma \cdot k)^2 (p_\gamma \cdot k') m^2 - 4m^2 (p_\gamma \cdot k')(p_\gamma \cdot k)(k \cdot k') + 2(p_\gamma \cdot k')^2 m^4 \Big],
\end{aligned}
\tag{23}
$$

$$
\begin{aligned}
C_2 = 2p_\gamma^0 k^0 \Big\{ &(p_\gamma \cdot k)^2 \big[(p_\gamma \cdot k') - m^2 \big] + (p_\gamma \cdot k')(p_\gamma \cdot k)(k \cdot k') \Big\} \\
&+ 2k'^0 k^0 \Big[-m^2 (p_\gamma \cdot k)^2 - m^2 (p_\gamma \cdot k')^2 \\
&+ (p_\gamma \cdot k')(p_\gamma \cdot k)\big\{ 2(k' \cdot k) + (p_\gamma \cdot k) - (p_\gamma \cdot k') \big\} \Big] \\
&+ 2p_\gamma^0 k'^0 \Big\{ (p_\gamma \cdot k')^2 \big[(p_\gamma \cdot k) + m^2 \big] - (p_\gamma \cdot k')(p_\gamma \cdot k)(k \cdot k') \Big\} \\
&+ 2(k'^0)^2 (p_\gamma \cdot k')(p_\gamma \cdot k)^2 - 2(k^0)^2 (p_\gamma \cdot k')^2 (p_\gamma \cdot k) \\
&- 2(p_\gamma^0)^2 (p_\gamma \cdot k')(p_\gamma \cdot k) m^2 + (p_\gamma \cdot k')^2 (k' \cdot k) m^2 \\
&- (p_\gamma \cdot k')^3 (p_\gamma \cdot k) + (p_\gamma \cdot k')^2 (p_\gamma \cdot k) m^2 - (p_\gamma \cdot k')^3 m^2 - (p_\gamma \cdot k')^2 m^4 \\
&- 2(p_\gamma \cdot k')(p_\gamma \cdot k)(k \cdot k')^2 - 2(p_\gamma \cdot k')(p_x \cdot k)^2 (k \cdot k') \\
&+ 2(p_\gamma \cdot k')^2 (p_\gamma \cdot k)(k \cdot k') + 2(p_\gamma \cdot k')(p_\gamma \cdot k)(k \cdot k') m^2
\end{aligned}
$$
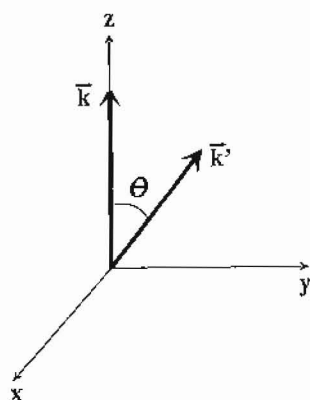
Fig. 6. Frame of reference in which the incoming electron is in the z direction and the outgoing electron is in the zy plane.

$$+ \left(p_\gamma \cdot k \right)^2 \left(k' \cdot k \right) m^2 - \left(p_\gamma \cdot k' \right) \left(p_\gamma \cdot k \right)^3$$
$$+ \left(p_\gamma \cdot k \right)^3 m^2 - \left(p_\gamma \cdot k' \right) \left(p_\gamma \cdot k \right)^2 m^2 - \left(p_\gamma \cdot k \right)^2 m^4 .$$

Alternatively we can write the cross section in terms of W_L and W_T as

$$\frac{\mathrm{d}^4\sigma}{\mathrm{d}\Omega_{\mathrm{out}} \, \mathrm{d}E_{\mathrm{out}} \, \mathrm{d}\Omega_\gamma \, \mathrm{d}E_\gamma} = \frac{\alpha^3 |k'| |p_\gamma|}{2\pi^2 |k| q^4 \left(p_\gamma \cdot k' \right)^2 \left(p_\gamma \cdot k \right)^2}$$
$$\times \left[-\frac{q^2}{|q|^2} W_L C_2 + W_T \left(-\frac{q^2}{|q|^2} C_2 + C_1 \right) \right]. \quad (24)$$

The expressions which we obtain are formally equivalent to those obtained in Ref. [12] in the study of radiative corrections to elastic and inelastic ep and μp scattering.

5. Results for incoherent bremsstrahlung

The calculations of this and the next sections are easily done in a frame of reference in which the incoming electron goes along the z direction and the outgoing electron is in the zy plane as shown in Fig. 6.

Thus

$$k = (0, 0, |k|),$$
$$k' = (0, |k'| \sin \theta, |k'| \cos \theta), \quad (25)$$

However, it is also useful to introduce a frame in which the momentum transfer $k - k'$ goes along the z direction as in Fig. 7, where p_γ is the photon momentum.
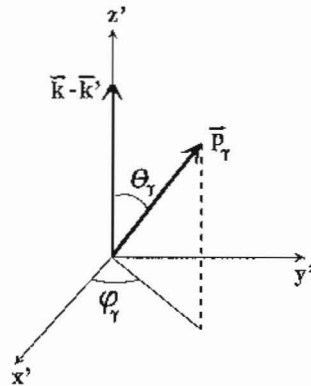
Fig. 7. Frame of reference in which the momentum transfer $k - k'$ is in the z direction and p_γ is the photon momentum.

In this latter frame of reference the p_γ components are given as

$$(p_\gamma)_{x'} = E_\gamma \sin \theta_\gamma \cos \phi_\gamma,$$
$$(p_\gamma)_{y'} = E_\gamma \sin \theta_\gamma \sin \phi_\gamma,$$
$$(p_\gamma)_{z'} = E_\gamma \cos \theta_\gamma. \tag{26}$$

One passes from the first frame to the second frame through a rotation of angle β along the x axis such that

$$\cos \beta = \frac{|k| - |k'| \cos \theta}{\sqrt{|k|^2 + |k'|^2 - 2|k||k'| \cos \theta}}, \tag{27}$$

and hence in the original frame the photon-momentum components are given by

$$p_\gamma(0) = E_\gamma,$$
$$p_\gamma(1) = E_\gamma \sin \theta_\gamma \cos \phi_\gamma,$$
$$p_\gamma(2) = E_\gamma(\cos \beta \sin \theta_\gamma \sin \phi_\gamma - \sin \beta \cos \theta_\gamma),$$
$$p_\gamma(3) = E_\gamma(\sin \beta \sin \theta_\gamma \sin \phi_\gamma + \cos \beta \cos \theta_\gamma). \tag{28}$$

In Figs. 8, 9, 10 we show some results for the IB cross section by fixing the incoming and outgoing electron energies and the angular variables of the photon. The results are plotted as a function of the (e, e') scattering angle for different energies of the incoming electron and different angles of the photon θ_γ.

We have no experimental data to compare our results with. It would however, be interesting to have such measurements and check that they have the structure of Eq. (24), with all the nuclear information contained in the response functions W_L, W_T, the same one as in the (e, e') inclusive process.

Our idea is to use this reaction as an alternative method to determine the response functions. In order to prove its adequacy for such purposes we imagine
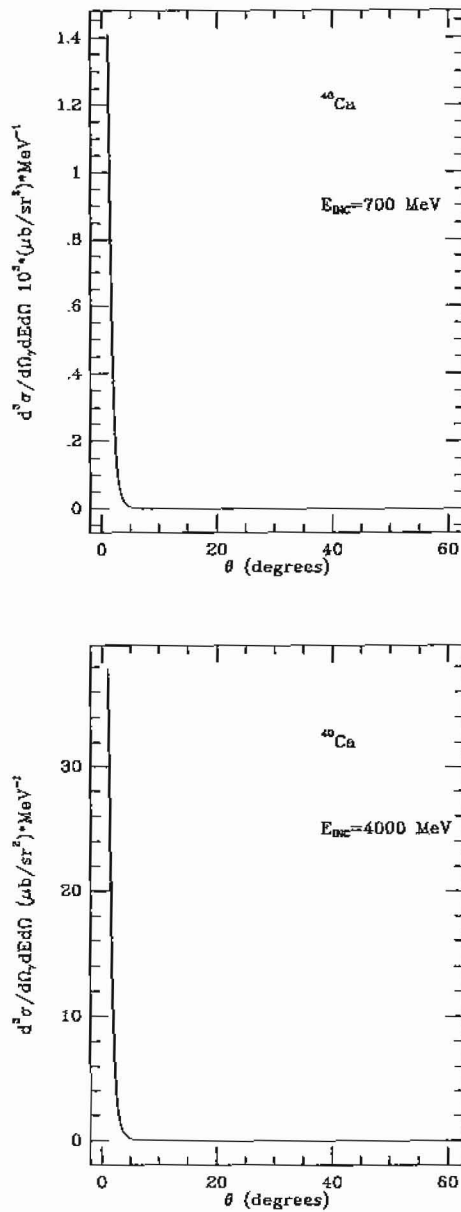
Fig. 8. IB cross section for ^{40}Ca by fixing: $E_{out} = \frac{1}{2}E_{inc}$, $\phi_\gamma = 40°$ and $\theta_\gamma = 2°$.

that the experiment is done, that the results obtained are those which we calculated and that we associate to them a certain experimental error. From the values of the cross sections in two different kinematical situations, giving rise to the same value of $|q|$ and ω for the argument of the response functions, we obtain
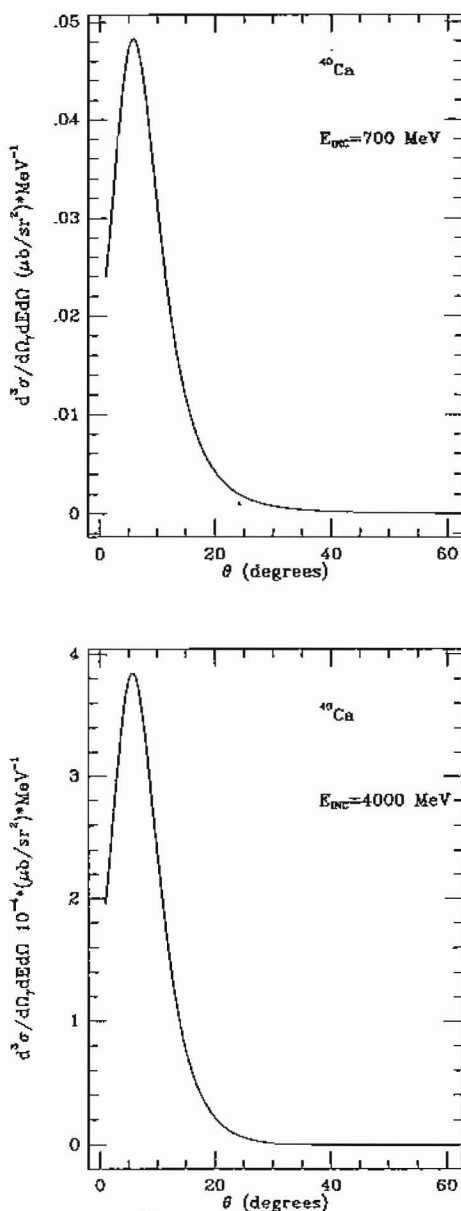
Fig. 9. IB cross section for ^{40}Ca by fixing: $E_{out} = \frac{1}{2}E_{inc}$, $\phi_\gamma = 40°$ and $\theta_\gamma = 15°$.

two independent equations which allow the determination of R_L and R_T with certain errors.

We have searched pairs of kinematical situations which lead to maximally independent equations or, equivalently, which induce minimum errors in R_L, R_T.
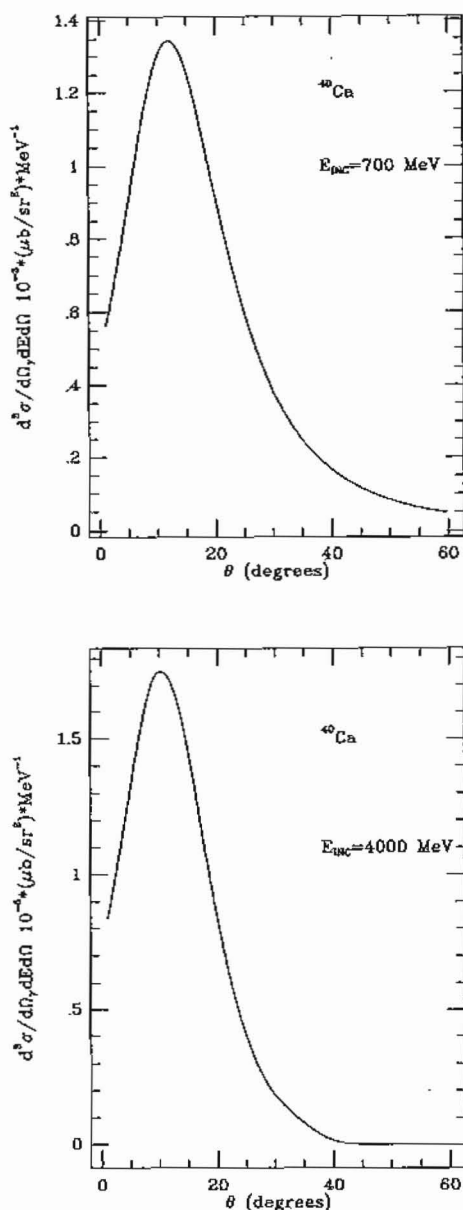
Fig. 10. IB cross section for ^{40}Ca by fixing: $E_{out} = \frac{1}{2}E_{inc}$, $\phi_\gamma = 40°$ and $\theta_\gamma = 30°$.

We have proceeded in the following way: we fix the initial electron energy and the angle ϕ_γ as specified in Fig. 7. Now for a given value of ω and $|q|$ we change the energy and the dispersion angle of the outgoing electron but in such a way as to minimize the errors induced in the determination of R_L, R_T. Following this

Table 1
$E_{inc} = 700$ MeV [a] and $|q| = 300$ MeV

ω (MeV)	W_L (MeV^{-1}) [b]	EW_L (MeV^{-1}) [c]	W_T (MeV^{-1}) [b]	EW_T (MeV^{-1}) [c]
31.9	8.6×10^{-2}	0.7×10^{-2}	2.54×10^{-2}	0.05×10^{-2}
41.9	0.126	0.011	3.65×10^{-2}	0.13×10^{-2}
51.9	0.153	0.013	4.40×10^{-2}	0.09×10^{-2}
61.9	0.159	0.013	4.54×10^{-2}	0.16×10^{-2}
71.9	0.139	0.012	3.94×10^{-2}	0.08×10^{-2}
81.9	0.115	0.09	3.22×10^{-2}	0.11×10^{-2}
91.9	8.8×10^{-2}	0.7×10^{-2}	2.45×10^{-2}	0.05×10^{-2}
101.9	6.1×10^{-2}	0.5×10^{-2}	1.69×10^{-2}	0.07×10^{-2}

[a] E_{inc}: energy of the incoming electron.
[b] W_L, W_T: longitudinal and transverse response functions.
[c] EW_L, EW_T: errors in the longitudinal and transverse response functions.

procedure we show in Table 1 the pairs of kinematical variables chosen to determine W_L, W_T at $|q| = 300$ MeV. For that purpose we take $E_{inc} = 700$ MeV and $\phi_\gamma = 40°$.

With the pairs of kinematical situations specified in Table 1 and assuming 5% errors in the experimental measurements of the cross sections we obtain the results for W_L, W_T shown in Table 2, with errors specified in the table.

We observe that the errors induced in W_L are of the order of 10% while those induced in W_T are of the order of 5% or less. As it is the case in the (e, e') experiments, the errors induced in the determination of R_L are larger than those in the determination of R_T. However, these errors can be placed under control with precise measurements of the cross section.

Our choice of pairs of kinematical situations to give maximally independent equations is not unique, many other pairs would give rise to similarly independent equations and it is not excluded that some other choice might even be better. However, one must be cautious in choosing the pairs of kinematical variables because there are many which lead to very large errors in the determination of W_L and W_T.

Table 2
$E_{inc} = 700$ MeV [a] and $|q| - 300$ MeV

ω (MeV)	E_{out} (MeV) [a]	θ_1 (deg)	θ_2 (deg)
31.9	140	10	170
41.9	140	10	156
51.9	130	10	170
61.9	130	10	156
71.9	120	10	170
81.9	140	10	154
91.9	130	10	170
101.9	110	10	152

[a] E_{inc}, E_{out}: energy of the incoming and outgoing electron.
[b] θ_1, θ_2: scattering-electron angles.

Table 3
$E_{inc} = 700$ MeV [a] and $|q| = 410$ MeV

ω (MeV)	W_L (MeV^{-1}) [b]	EW_L (MeV^{-1}) [c]	W_T (MeV^{-1}) [b]	EW_T (MeV^{-1}) [c]
31.9	2.5×10^{-2}	0.3×10^{-2}	1.39×10^{-2}	0.03×10^{-2}
41.9	3.5×10^{-2}	0.4×10^{-2}	1.89×10^{-2}	0.03×10^{-2}
51.9	4.5×10^{-2}	0.5×10^{-2}	2.40×10^{-2}	0.05×10^{-2}
61.9	5.4×10^{-2}	0.6×10^{-2}	2.87×10^{-2}	0.05×10^{-2}
71.9	6.4×10^{-2}	0.8×10^{-2}	3.35×10^{-2}	0.06×10^{-2}
81.9	7.4×10^{-2}	0.9×10^{-2}	3.86×10^{-2}	0.07×10^{-2}
91.9	8.2×10^{-2}	0.9×10^{-2}	4.22×10^{-2}	0.07×10^{-2}
101.9	8.3×10^{-2}	0.9×10^{-2}	4.22×10^{-2}	0.07×10^{-2}

[a] E_{inc}: energy of the incoming electron.

[b] W_L, W_T: longitudinal and transverse response functions.

[c] EW_L, EW_T: error in the longitudinal and transverse response functions.

Table 4
$E_{inc} = 700$ MeV [a] and $|q| = 410$ MeV

ω (MeV)	E_{out} (MeV) [a]	θ_1 (deg)	θ_2 (deg)
31.9	200	28	158
41.9	190	28	170
51.9	190	24	160
61.9	180	28	170
71.9	180	28	158
81.9	170	28	170
91.9	170	22	158
101.9	160	28	170

[a] E_{inc}, E_{out}: energy of the incoming and outgoing electron.

[b] θ_1, θ_2: scattering-electron angles.

In Tables 3 and 4 we show similar results as in Tables 1, 2 leading to the determination of the response functions at $|q| = 410$ MeV. The relative errors are similar as in the case of the former tables.

6. Comparison of coherent and incoherent bremsstrahlung

In this section we compare the results of the CB and IB in order to see when the contribution of the IB becomes comparable or larger than the one from the CB, thus invalidating the assumptions made in the tagging technique. For this purpose we assume that the photon is emitted in the direction of the momentum transfer $k - k'$ (the one which maximizes the CB) and then look at the cross section as a function of the electron-dispersion angle.

In Figs. 11, 12, 13 we have taken different energies of the incoming electron and chosen the energy of the outgoing electron to be $\frac{3}{4}$ of the electron energy. In the
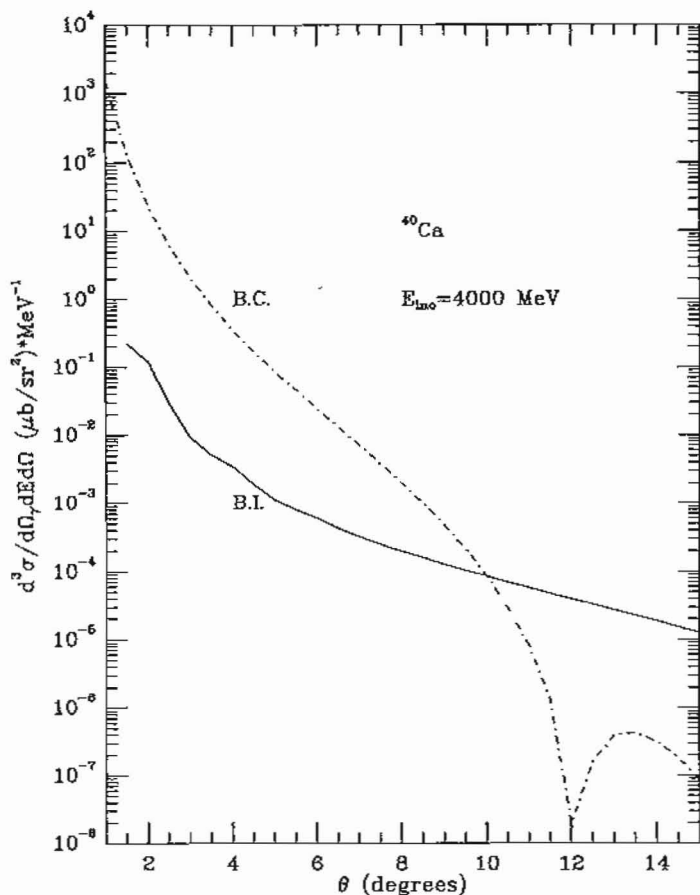
Fig. 11. Comparison between IB and CB cross sections for ^{40}Ca by fixing: $E_{inc} = 4000$ MeV, $E_{out} = \frac{3}{4}E_{inc}$, $\phi_\gamma = 40°$ and $\theta_\gamma = 0°$.

CB this forces $E_\gamma = \frac{1}{4}E_{inc}$, but in the IB one must integrate over all possible energies of the photon ($E_\gamma \neq 0$) since this is a free variable in this process. What we observe in the figures is that at small e^- dispersion angles the CB dominates over the IB but at larger angles the IB dominates the CB. We also observe that as the energy of the e^- beam increases, the region of dominance of the CB over the IB is moved to smaller angles. For E_{inc} energies around 20 GeV the region of dominance of CB over IB is limited to scattering angles smaller than 5°. Our results also show that for e^- energies of the order of 1 GeV the dominance of the CB over the IB extents to relatively large angles of the scattering angle, thus making absolutely safe the tagging technique to obtain monochromatic photons as presently done.

7. Conclusion

The study done in this paper has served two purposes. In the first place we have shown that the process of incoherent bremsstrahlung can be used as a source of information to extract the nuclear response functions. It is possible to measure the cross sections in different pairs of kinematical situations such that with two equations we determine W_T with relative errors typically of the order of the experimental one of the cross section, while W_L can be determined with relative errors of the order of double that amount. This is sufficiently good for accurate determinations of W_L and W_T. Given the large discrepancies in W_L obtained in different experiments using the (e, e') reaction, the exploration of alternative methods like the one we propose here becomes advisable.
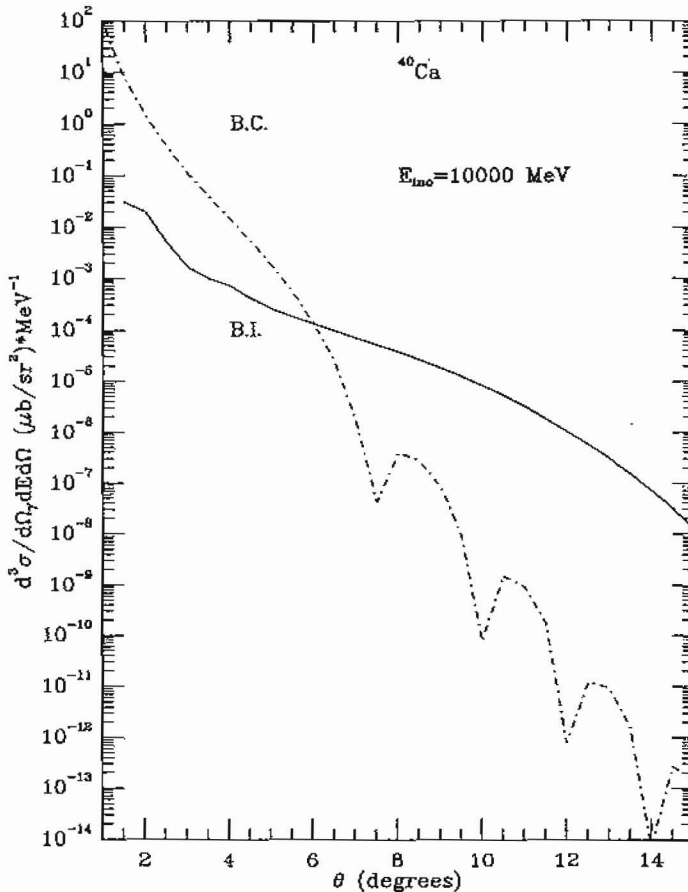
Fig. 12. Comparison between IB and CB cross sections for ^{40}Ca by fixing: $E_{inc} = 10000$ MeV, $E_{out} = \frac{3}{4} E_{inc}$, $\phi_\gamma = 40°$ and $\theta_\gamma = 0°$.
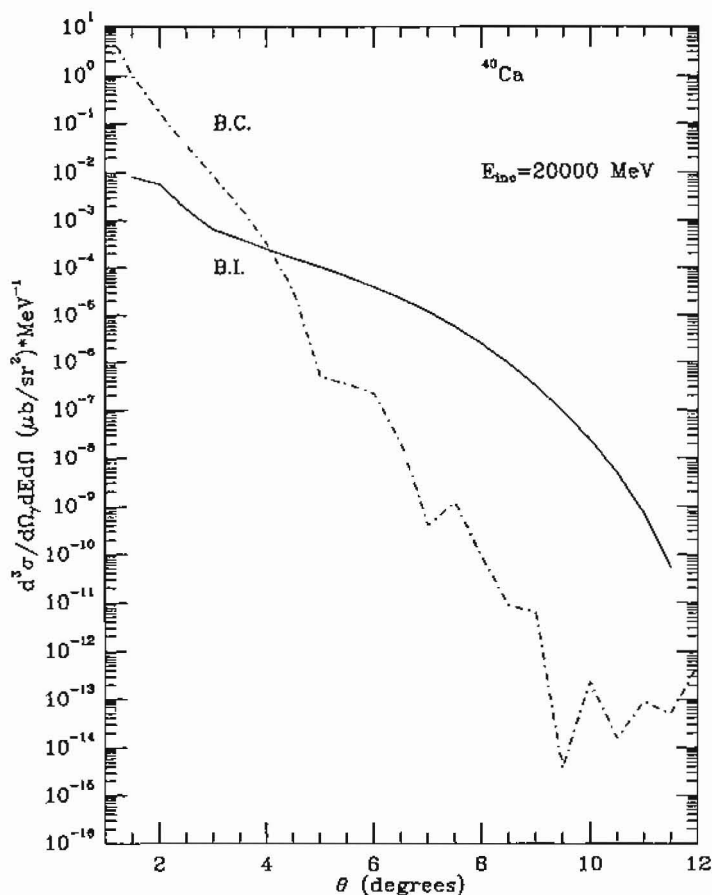
Fig. 13. Comparison between IB and CB cross sections for ^{40}Ca by fixing: $E_{inc} = 20000$ MeV, $E_{out} = \frac{1}{4}$ E_{inc}, $\phi_\gamma = 40°$ and $\theta_\gamma = 0°$.

On the other hand we have compared the coherent bremsstrahlung with the incoherent one in order to see the limits to the tagging technique which assumes absolute dominance of the coherent process. We observed that for energies of the present intermediate-energy-electron machines, $E_e < 1$ GeV, the CB dominates the IB even at e^- scattering angles bigger than 20°, making absolutely safe the tagging technique to produce monochromatic photon as currently done. However, as we increase the energy of the electron, the region of dominance of the CB versus IB is reduced to smaller scattering angles. At energies of around 20 GeV this region is reduced to scattering angles smaller than 5°. The present results should be of use to set the limits of the tagging technique in some of the planned or future electron facilities.

References

[1] T.C. Yates et al., Phys. Lett. B 312 (1993) 382.
[2] Z.E. Meziani et al., Nucl. Phys. A 446 (1985) 113; Phys. Rev. 52 (1984) 2130; 54 (1985) 1123.
[3] K.K. Seth, private communication.
[4] C. Itzykson and B. Zuber, Quantum field theory (McGraw Hill, New York, 1980).
[5] F. Mandl and G. Shaw, Quantum field theory (Wiley, New York, 1984).
[6] E. Amaldi, S. Fubini and G. Furlan, Pion electroproduction, Springer tracts in modern physics, Vol. 83 (Springer, Berlin, 1979).
[7] P.J. Mulders, Phys. Reports 185 (1990) 83.
[8] S. Nozawa and T.-S.H. Lee, Nucl. Phys. A 513 (1990) 511.
[9] W. Alberico et al., Phys. Rev. C 381 (1988) 1801.
[10] H.C. Chiang, E. Oset and P. Fernández de Córdoba, Nucl. Phys. A 510 (1990) 591.
[11] S.K. Singh and E. Oset, Nucl. Phys. A 542 (1992) 587; Phys. Rev. C 48 (1993) 1246.
[12] L.W. Mo and Y.S. Tsai, Rev. Mod. Phys. 41 (1969) 205.